

Bipolarons in the Extended Holstein Hubbard Model

^aJ. Bonča and ^bS. A. Trugman

^a FMF, University of Ljubljana and J. Stefan Institute, 1000, Slovenia,

^bTheory Division, Los Alamos National Laboratory, Los Alamos, NM 87545,

(October 29, 2018)

We numerically and analytically calculate the properties of the bipolaron in an extended Hubbard Holstein model, which has a longer range electron-phonon coupling like the Fröhlich model. In the strong coupling regime, the effective mass of the bipolaron in the extended model is much smaller than the Holstein bipolaron mass. In contrast to the Holstein bipolaron, the bipolaron in the extended model has a lower binding energy and remains bound with substantial binding energy even in the large- U limit. In comparison with the Holstein model where only a singlet bipolaron is bound, in the extended Holstein model a triplet bipolaron can also form a bound state. We discuss the possibility of phase separation in the case of finite electron doping.

PACS: 74.20.Mn, 71.38.+i, 74.25.Kc

There is growing evidence that electron-phonon coupling plays an important role in determining exotic properties of novel materials such as colossal magnetoresistance [1] and high- T_c compounds [2]. Since electrons in these materials are strongly correlated, the interplay between an attractive electron phonon interaction and Coulomb repulsion may be important in determining physics at finite doping. In particular, when the electron-phonon interaction is local, as is the case in the Holstein model, finite Coulomb repulsion leads to the formation of an intra-site bipolaron [3–5], with an effective mass of the order of the polaron effective mass [5].

It has been recently discovered that a longer-range electron-phonon interaction leads to a decrease in the effective mass of a polaron in the strong-coupling regime [6,7]. The lower mass can have important consequences, because lighter polarons and bipolarons are more likely to remain mobile, and less likely to trap on impurities or from mutual repulsion. Motivated by this discovery, we investigate a simplified version of the Fröhlich model in the case of two electrons,

$$\begin{aligned}
 H = & -t \sum_{js} (c_{j+1,s}^\dagger c_{j,s} + H.c.) \\
 & - \omega g_0 \sum_{jls} f_l(j) c_{j,s}^\dagger c_{j,s} (a_l + a_l^\dagger) \\
 & + \omega \sum_j a_j^\dagger a_j + U \sum_j n_{j\uparrow} n_{j\downarrow},
 \end{aligned} \quad (1)$$

where $c_{j,s}^\dagger$ creates an electron of spin s and a_j^\dagger creates a phonon on site j . The second term represents the coupling of an electron on site j with an ion on site l , where g_0 is the dimensionless electron-phonon coupling constant. While in general long range electron-phonon coupling $f_l(j)$ is considered [6,7], we further simplify this model by placing ions in the interstitial sites located between Wannier orbitals, as occurs in certain oxides [8], shown in Fig. (1a). In this case it is natural to investigate a simplified model, where an electron located on site

j couples only to its two neighboring ions, *i.e.* $l = j \pm 1/2$. We describe such coupling with $f_{j \pm 1/2}(j) = 1$ and 0 otherwise, and refer to this model as the extended Holstein Hubbard model (EHHM). We can view the EHHM as the simplest model with longer range than a single site, and use it to explore the qualitative change in physics in the simplest possible setting. While it is clear that in comparison to the Fröhlich model, our simplified EHHM lacks long range tails in the electron phonon interaction, the physical properties that depend predominantly on the short range interaction should be similar. For example, calculating the polaron energy of the original Fröhlich model as defined in Refs. [6,7], one finds that 94% of the total polaron energy comes from the first two sites.

In the case when $f_l(j) = \delta_{l,j}$, the model in Eq. (1) maps onto a Holstein-Hubbard model (HHM) (see also Fig.(1b)). The last two terms in Eq. (1) represent the energy of the Einstein oscillator with frequency ω and the on-site Coulomb repulsion between two electrons. We consider the case where two electrons with opposite spins ($S_z = 0$) couple to dispersionless optical phonons with polarization perpendicular to the chain.

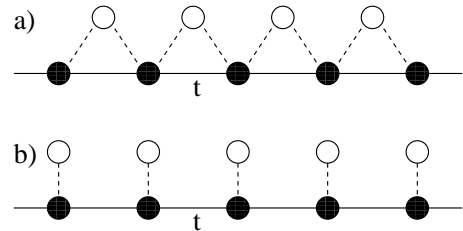


FIG. 1. Schematic representation of the simplified a) extended Holstein and b) Holstein model on a chain. Filled circles represent electron Wannier orbitals, open circles represent ions. Solid lines indicate overlap integral t between Wannier orbitals, dashed lines represent nonzero electron-phonon coupling.

In this Letter we use a recently developed, highly accurate numerical technique [9,5], combined with a strong

coupling expansion to study the simplified EHHM. Our main goal is to calculate physical properties such as the binding energy, effective mass, isotope effect, and the phase diagram of the EHHM bipolaron and compare them to the Holstein bipolaron that has been thoroughly studied recently [5]. Even though the two models appear very similar, we find profound differences between the physical properties of bipolarons within the EHHM and the HHM.

The numerical method that we use creates a systematically expandable variational space of phonon excitations in the vicinity of the two electrons [9,5]. The variational method is defined on an infinite lattice and is not subject to finite-size effects. It allows the calculation of physical properties at any wavevector k . In the intermediate coupling regime where it is most accurate, it provides results that are variational in the thermodynamic limit and gives energies accurate to 14 digits for the polaron case and up to 7 digits for the bipolaron case.

To investigate the strong coupling regime of the EHHM, we use a Lang-Firsov [10] unitary transformation $\tilde{H} = e^S H e^{-S}$, where $S = g_0 \sum_{jls} f_l(j) n_{js} (a_l - a_l^\dagger)$. This incorporates the exact distortion and interaction energies for static electrons into H_0 , and leads to a transformed Hamiltonian

$$\begin{aligned} \tilde{H} &= H_0 + T, \\ H_0 &= \omega \sum_j a_j^\dagger a_j - \omega g_0^2 \sum_{ijl} f_l(i) f_l(j) n_i n_j + U \sum_j n_{j\uparrow} n_{j\downarrow}, \\ T &= -t e^{-\tilde{g}^2} \sum_{js} c_{j+1,s}^\dagger c_{j,s} e^{-g_0 \sum_l (f_l(j+1) - f_l(j)) a_l^\dagger} \\ &\quad e^{g_0 \sum_l (f_l(j+1) - f_l(j)) a_l} + \text{H.c.}, \end{aligned} \quad (2)$$

where $n_j = n_{j\uparrow} + n_{j\downarrow}$ and $\tilde{g}^2 = g_0^2 \sum_l [f_l(0)^2 - f_l(0) f_l(1)]$; $\tilde{g} = g_0$ for the EHHM. The second term in H_0 gives the polaron energy, which in the EHHM case is $\epsilon_p = 2\omega g_0^2$, while for the HHM, $\epsilon_p = \omega g_0^2$. This term also includes the interaction between electrons located on neighboring sites, a consequence of the non-local electron-phonon interaction. As noted by Alexandrov and Kornilovitch [6], in the strong coupling regime a Fröhlich polaron has a much smaller effective mass than a Holstein polaron with the same polaron energy ϵ_p . The reason for lower mass in the Fröhlich case (as well as EHHM) is that the effective electron-phonon coupling that renormalizes hopping $\tilde{g}^2 = \gamma \epsilon_p / \omega$ is smaller (in EHHM, $\gamma = 1/2$) than in the case of the HHM with $\gamma = 1$. In the strong coupling EHHM polaron, the phonon is displaced on two sites. It is identical on one of these sites in the initial and the final state after the electron hop, resulting in a smaller mass enhancement from phonon overlap.

In the anti-adiabatic limit where $g_0 \rightarrow 0$ and $\omega \rightarrow \infty$ with ωg_0^2 constant, the phonon interaction is instantaneous and our simplified EHHM model maps onto a generalized Hubbard model

$$\begin{aligned} H &= -t \sum_{js} (c_{j+1,s}^\dagger c_{j,s} + \text{H.c.}) \\ &\quad + \tilde{U} \sum_j n_{j\uparrow} n_{j\downarrow} + V \sum_j n_j n_{j+1}, \end{aligned} \quad (3)$$

with an effective Hubbard interaction $\tilde{U} = U - 4\omega g_0^2$ and $V = -2\omega g_0^2$. In the case of two electrons an analytical solution can be found. As many as three bound states may exist: two singlets and a triplet. In the case when $U = 0$ there is always at least one singlet bound state. A triplet bound state with an energy $E = -2\omega g_0^2 - 2t^2/\omega g_0^2$ exists only when $\omega g_0^2 > t$.

In the strong coupling limit, T in Eq. (2) may be considered as a perturbation. In the case when $U < 2\omega g_0^2$, the single site or S0 bipolaron, defined as $\phi_{S0} = c_{0\uparrow}^\dagger c_{0\downarrow}^\dagger |0\rangle$, has the lowest energy to zeroth order. In this regime the binding energy is $\Delta = E_{bi}^{S0} - 2\epsilon_p = U - 4\omega g_0^2$, where E_{bi}^{S0} denotes the S0 bipolaron energy and ϵ_p is the energy of a polaron in zeroth order. In the opposite regime, when $U > 2\omega g_0^2$, the inter-site or S1 bipolaron, $\phi_{S1}^{S=0,1} = \frac{1}{\sqrt{2}} (c_{0\uparrow}^\dagger c_{1\downarrow}^\dagger \pm c_{0\downarrow}^\dagger c_{1\uparrow}^\dagger) |0\rangle$, has the lowest energy. Its binding energy $\Delta = -2\omega g_0^2$ does not depend on U , which also leads to a degeneracy between the spin-singlet (S=0) and the spin-triplet (S=1) state. This simple analysis predicts that a EHHM bipolaron (EHB) remains bound in the strong coupling regime even in the limit when $U \rightarrow \infty$.

It is worth stressing that in the limit $U \rightarrow \infty$, singlet and triplet bipolarons become degenerate. We can therefore predict the existence of a singlet and a triplet bipolaron, where at finite U the singlet bipolaron has lower energy. It is also obvious that the energy of the triplet bipolaron should not depend on U . In contrast to these predictions, a triplet Holstein bipolaron (HB) is never stable, and furthermore in the limit $U \rightarrow \infty$ no bound HB exists [5].

Next, we focus on the effective mass of the EHB in the strong coupling regime. First order perturbation theory does not lead to energy corrections for the S0 EHB. Second order perturbation theory gives

$$m_{S0}^{*-1} = 4t^2 e^{-2g^2} \sum_{n=0} \frac{(-2g^2)^n}{n!} \frac{1}{\epsilon_p - U + n\omega}, \quad (4)$$

where $m^{*-1} \equiv d^2 E(k)/dk^2$. Equation (4) is only valid in the limit when $1/\lambda \equiv 2t/\epsilon_p \rightarrow 0$ and $U \ll \epsilon_p$. In the limit of large g and $U = 0$, $m_{S0}^* \propto \exp(2\epsilon_p/\omega)$, which should be compared to the HB effective mass that scales as $m_{S0}^* \propto \exp(4\epsilon_p/\omega)$ [5,11]. In the strong coupling regime the EHB should be much lighter than the Holstein bipolaron. There is a particularly interesting EHB regime when $U = \epsilon_p$. In this case the zero order energies of the ϕ_{S0} and $\phi_{S1}^{S=0,1}$ bipolarons are degenerate. Degenerate first order perturbation theory can be applied to the spin-singlet EHB in this case, which leads to a substantial decrease in the effective mass

$$m_{EHB}^*(U = \epsilon_p) = \frac{\sqrt{2}}{t} e^{\epsilon_p/2\omega}. \quad (5)$$

The EHB in this regime consists of a superposition of ϕ_{S0} and $\phi_{S1}^{S=0}$, and moves through the lattice in a crab-like motion. Its binding energy is $\Delta = -\epsilon_p - 2\sqrt{2}t \exp(-\epsilon_p/2\omega)$.

In the $U \rightarrow \infty$ limit we apply the second-order perturbation theory to the S1 bipolaron. We take into account processes where one of the electrons within the S1 bipolaron jumps to the left (right) and then the other follows. This leads to

$$m_{EHB}^*(U = \infty) = \frac{\lambda}{t} e^{\epsilon_p/\omega}. \quad (6)$$

Strong coupling approach thus predicts nonmonotonous dependence of the effective EHB mass as a function of U as can be seen from different exponents in Eqs. (4,5,6).

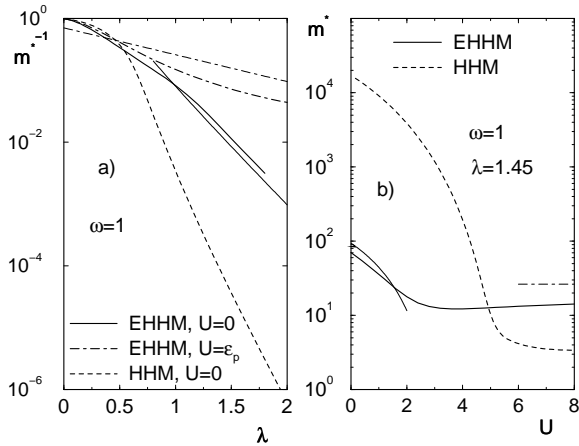


FIG. 2. a) The bipolaron inverse effective mass vs. λ at $\omega = 1$. The thin full line and thin dot-dashed line represent strong coupling results obtained using Eqs. (4) and (5) respectively. b) The effective mass vs. U at $\omega = 1$ and $\lambda = 1.45$. The thin full and dot-dashed lines represent strong coupling results obtained using Eqs. (4) and (6) respectively.

We next present numerical results. To achieve sufficient accuracy, we have used up to 3×10^6 variational states. We use units where the bare hopping constant is $t = 1$. The ground state energy of the EHB at $\lambda = 0.5$, $\omega = U = 1$, is $E = -5.822621$, which is accurate to the number of digits shown. (For the same parameters, $U = 0$, the Holstein bipolaron energy is $E = -5.4246528$.) The accuracy of our plotted results in the thermodynamic limit is well within the line-thickness. In Fig. (2a) we present the inverse effective masses of the EHB and the HB at $U = 0$ and of the EHB at $U = \epsilon_p$. Our results for the bipolaron mass are in qualitative agreement with results for the polaron effective mass by Alexandrov and Kornilovitch [6]. In the weak coupling regime we find the EHB slightly heavier than

the HB, while in the strong coupling regime the opposite is true. Setting the Coulomb interaction to $U = \epsilon_p$, the effective mass becomes even lighter, which is a consequence of the smaller exponent in Eq. (5). In the strong coupling regime ($\lambda \geq 1$), we find good agreement with our strong coupling predictions in Eqs. (4,5), depicted by thin lines. While the absolute values may differ by up to a factor of 4 (in the case of $U = \epsilon_p$), the strong coupling approach almost perfectly predicts the exponential dependence (seen as parallel straight lines in Fig. (2a)) of the effective masses on $\epsilon_p = 2t\lambda$.

To obtain better understanding of the effect of on-site Coulomb repulsion on the bipolaron effective mass in the strong coupling regime, we present in Fig. (2b) effective masses of the EHB and HB at fixed coupling strength $\lambda = 1.45$ as a function of U . The most prominent finding is that the EHB is two orders of magnitude lighter than the HB when $U = 0$. While the effective mass of the HB decreases monotonously with U , the EHB effective mass reaches a shallow minimum near $U = \epsilon_p$ as predicted by the strong coupling approach. At larger $U > \epsilon_p$ we observe a slight increase in the effective mass. In the same regime HB effective mass drops below EHB effective mass. This crossing coincides with a substantial decrease of the HB binding energy and consequently with separating of HB into two separate polarons. Numerical results for the EHB agree reasonably well with analytical predictions for small U , Eq. (4), and also in the limit of large U , Eq. (6).

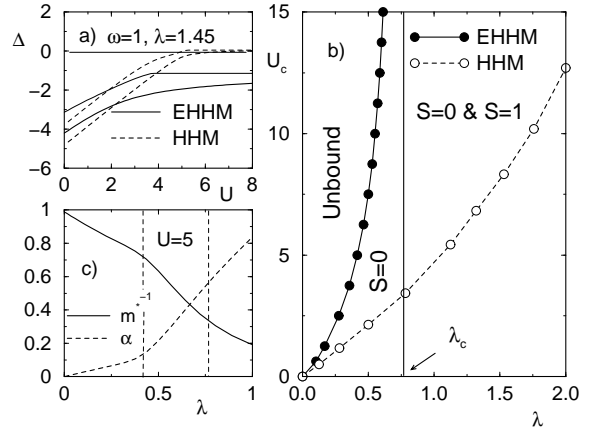


FIG. 3. a) Binding energies $\Delta^{(0,1)}$ vs. U of the EHHM (full lines) and the HHM (dashed lines). Corresponding binding energies of the first excited states are indicated with thin lines. b) Phase diagram of the EHHM (filled circles) and the HHM (open circles) calculated at $\omega = 1$. The vertical line at $\lambda = \lambda_c$ represents the stability line of the $S = 1$ EHB. Text in the figure applies only to EHHM phase diagram. c) The inverse effective mass and the isotope effect of the EHHM vs. λ at $U = 5$. Vertical lines represent stability limits of the $S = 0$ and $S = 1$ EHB (from left to right).

To gain an insight into the symmetry of the bound

EHB state, we have calculated the binding energy $\Delta^{(0,1)} = E_{bi}^{(0,1)} - 2E_{po}$ where $E_{bi}^{(0,1)}$ are the ground state and the first excited energy of the EHHM or HHM for two electrons with opposite spins, $S_z = 0$, and E_{po} is the ground state energy of the corresponding model with one electron. In Fig. (3a) we present binding energies of the bipolaron ground and first excited states as a function of U . An important difference between the HHM and the EHHM is that in the former case a critical U_c exists for any coupling strength λ when the HB unbinds, while the EHB remains bound even in the limit $U \rightarrow \infty$ when $\lambda > \lambda_c = 0.76$. At small U excited states of both models correspond to bipolaronic singlets, spaced approximately ω above the ground state. Singlets can be recognized by the fact that their binding energies depend on U . As U increases, the excited state of the HB unbinds while the excited state of the EHB undergoes a transition from a singlet to a triplet state which is also bound.

By solving $\Delta^{(0,1)}(\lambda, U_c) = 0$ we arrive at the phase diagram (U_c, λ) of the EHHM calculated at fixed $\omega = 1$, presented in Fig. (3b). We indicate three different regimes. For small λ and large U no bound bipolarons exist. With increasing λ there is a phase transition into a bound singlet bipolaron state. Increasing λ even further, a triplet bipolaron becomes bound as well at $\lambda = \lambda_c$. For comparison we also include the phase boundary of the HHM (open circles). Note that only a singlet bipolaron exists in the HHM.

In Fig. (3c) we present a cross section through the phase diagram in Fig. (3b) at fixed $U = 5$, and plot m^{*-1} and the isotope effect $\alpha \equiv d \ln m_{bi} / d \ln M$ vs. λ (see also discussion of the isotope effect in Ref. [5]). The effective mass increases by approximately a factor of 2.5 from its noninteracting value in the regime where only a spin-singlet bipolaron exists (between the two vertical dashed lines). The increase of the effective mass is followed by an increase in the isotope effect. The binding energy (not plotted) reaches a value $\Delta \sim -0.5t$ at $\lambda = \lambda_c = 0.76$.

To conclude, we have shown that a light EHB exists even in the strong coupling regime with an effective mass that can be a few orders of magnitude smaller than the HB effective mass at small U . At finite $U = \epsilon_p$ a regime of extremely light EHB is found where bipolaron effective mass scales with the same exponent as the polaron effective mass. This mobile bipolaron arises as a superposition of a ϕ_{S0} and a ϕ_{S1} state and it moves through a lattice in a crab-like motion. As found in ref. [5], HB becomes very light with increasing U close to the transition into two unbound polarons at $U = U_c$. Near this transition, its binding energy diminishes substantially and reaches $\Delta = 0$ at the transition point U_c . In contrast, EHB can have a small effective mass even in the regime where its binding energy is large (in the strong coupling regime Δ approaches $\Delta = -\epsilon_p$). Furthermore, EHB remains bound in the limit when $U \rightarrow \infty$. As a consequence of a

longer-range electron-phonon interaction, a bound spin-triplet bipolaron exists in the EHHM for $\lambda > \lambda_c$. The difference between the binding energies of the spin-singlet and the spin-triplet bipolaron is proportional to $1/U$. In the weak to intermediate coupling regime of the EHHM ($\lambda < \lambda_c$ and finite U) $S = 0$ bipolarons exist with substantial binding energy close to $\lambda \sim \lambda_c$, and an effective mass of the order of noninteracting electron mass.

The existence of a singlet and a triplet EHB state has important implications in the case of finite doping. As was established previously, there is no phase separation in the low-density limit of the HHM despite a substantially renormalized bandwidth [5]. The reason is in part that a triplet bipolaron is always unstable. The lack of phase separation in the low-density limit and in the strong coupling regime has a simple intuitive explanation: a third particle, added to a bound singlet bipolaron, introduces a triplet component to the wavefunction. The opposite is true in the strong coupling limit of EHHM where singlet and triplet bipolarons coexist. In this case, the third added particle simply attaches to the existing singlet bipolaron and thus gains in the potential energy. We therefore expect that the EHHM phase separates in the case of finite doping for λ sufficiently large. To stabilize a system of EHHM bipolarons against phase separation, a long-range Coulomb repulsion should be taken into account. This prediction is in agreement with recent findings by Alexandrov and Kabanov [12] that state, that there is no phase segregation in the Fröhlich model in the presence of long-range Coulomb interactions.

J.B. gratefully acknowledges the support of Los Alamos National Laboratory where part of this work has been performed, and financial support by the Slovene Ministry of Science, Education and Sport. This work was supported in part by the US DOE.

-
- [1] S. Jin *et al.*, *Science* **264**, 413 (1994).
 - [2] J.G. Bednorz and K.A. Müller, *Z. Phys. B* **64**, 189 (1986).
 - [3] L. Proville and S. Aubry, *Physica D* **133**, 307 (1998); *Eur. Phys. J. B* **11**, 41 (1999).
 - [4] H. Fehske, H. Röder, G. Wellein, and A. Mistryotis, *Phys. Rev. B* **51**, 16582 (1995).
 - [5] J. Bonča, T. Katrašnik, and S. A. Trugman, *Phys. Rev. Lett.* **84**, 3153 (2000).
 - [6] A.S. Alexandrov and P.E. Kornilovitch, *Phys. Rev. Lett.* **82**, 807 (1999).
 - [7] H. Fehske, J. Loos, and G. Wellein, *Phys. Rev. B* **61**, 8016 (2000).
 - [8] N. Tsuda, K. Nasu, A. Yanase, and K. Siratori, *Electronic Conduction in Oxides*, Springer-Verlag (1991).
 - [9] J. Bonča, S. A. Trugman and I. Batistič, *Phys. Rev. B* **60**, 1633 (1999).

- [10] I. G. Lang and Yu. A. Firsov, Sov. Phys. JETP **16**, 1301 (1963); Sov. Phys. Solid State **5**, 2049 (1964).
- [11] A.S. Alexandrov and V.V. Kabanov, Sov. Phys. Solid State **28**, 631 (1986).
- [12] A.S. Alexandrov and V.V. Kabanov, JETP Lett. **72**, 569 (2000).